Influence of β-Sheet Structure on the Susceptibility of Proteins to Backbone Oxidative Damage: Preference for αC-Centered Radical Formation at Glycine Residues of Antiparallel β-Sheets

Arvi Rauk* and David A. Armstrong

Contribution from the Department of Chemistry, University of Calgary, Calgary, AB, Canada, T2N 1N4

Received November 10, 1999. Revised Manuscript Received February 17, 2000

Abstract: Ab initio calculations at the B3LYP/6-31G(d) level of theory were carried out on selected cyclic hydrogen-bonded (H-bonded) dimers of glycine and alanine as models for β-sheets and on the αC-centered radicals derived from them. The structures mirrored the cycles found in the H-bonded network of parallel and antiparallel β-sheet secondary structure, and were otimized both with and without enforcement of constraints on the Φ,Ψ torsion angles. Transition structures for the migration of an H atom from an αC site to another αC site or to an S atom were located. It was found that the presence of a H-bonded strand of a β-sheet has little effect on the αC−H bond dissociation enthalpy (BDE) of glycine but raises the BDE of other residues by a significant amount. The *parallel* β-sheet structure and Φ,Ψ angles lead to a significant increase in BDE, relative to the random coil structure, due to loss of captodative stabilization. The *antiparallel* β-sheet structure and Φ,Ψ angles do not lead to a significant increase in BDE. All residues incorporated in β-sheet secondary structure, with the exception of glycine, are protected from oxidative damage because the αC−H bond is internal to the sheet and inaccessible to oxidizing radicals. Glycine is susceptible to oxidative damage because it has a second αC−H bond which is exposed. Among residues in secondary structures, only glycine is susceptible to damage by weak oxidants such as thiyl radicals and superoxide, provided it is in an antiparallel β-sheet. Radical damage may propagate readily from one strand to another above the β-sheet, but not within the β-sheet. β-Sheet structure narrows the difference between the glycyl αC−H BDE and S−H BDE and facilitates interstrand H atom transfer between the glycyl αC site and the S atom of cysteine.

Introduction

In the past decade there has been a rapid growth of interest in free radicals in proteins. Except in a few cases,[1] such radicals arise from the action of more reactive oxidizing radical species (ROS). ROS are generated as a result of "mistakes" in the normal metabolic functions having to do with oxygen transport in red blood cells and its reduction in mitochondria,[2,3] in the detoxification of extraneous chemicals in the liver,[3,4] and through ionizing radiation.[5] The probability of the formation of free radicals in proteins depends on two factors, thermochemistry and opportunity. In other words, reactions that produce free radicals should be exothermic (or if endothermic, by not more than a few kJ mol^{-1}), and hindered by modest activation barriers else the reactions would be too slow to be of physiological importance. Second, the reagents must be able to achieve the geometry required for the transition state for the reaction, an important primary requirement being that they can get together in the first place. Hitherto, we have focused our attention on backbone radicals of the polypeptide chain, since such radicals are captodatively stabilized.[6,7] Consequently, thermochemistry provides no barrier to strong oxidizing species such as hydroxyl or alkoxyl radicals, and even weaker oxydizing species such as superoxide ($O_2^{\bullet-}$)/hydroperoxyl ($HOO^{\bullet}$) and thiyl radicals ($RS^{\bullet}$) can abstract a hydrogen atom from an αC site in an exothermic reaction. The consequences of formation of such αC-centered radicals have been widely discussed.[8−10] Under normal aerobic conditions such radicals react rapidly with dissolved molecular oxygen leading to the formation of superoxide and/or hydroperoxides and ultimately to the rupture of the protein backbone.

The stability of αC-centered radicals depends on the particular residue under attack and could be measured by the strength of the αC−H bond. However, no bond dissociation enthalpies (BDEs) of αC−H bonds are available experimentally. Modern theoretical/computational techniques are now able to provide structures and energies of model peptides which are large enough to reflect the local protein environment. We have initially used these methods to obtain values of D_{CH}, the BDE at 298 K, for the residues of glycine[7] and the amino acids with smaller aliphatic side chains: alanine, serine, threonine,[11]

* To whom correspondence should be addressed.

(1) Stubbe, J.; van der Donk, W. A. *Chem. Rev.* **1998**, *98*, 705−762.

(2) (a) Simic, M. G., Taylor, K. A., Ward, J. F., von Sonntag, C., Eds. *Oxygen Radicals in Biology and Medicine*; Plenum Press: New York, 1988. (b) Sies, H., Ed. *Oxidative Stress − Oxidants and Anti-Oxidants*; Academic Press: London, 1991.

(3) Davies, K. J. A., Ed. *Oxidative Damage and Repair: Chemical, Biological and Medical Aspects*; Pergamon Press: New York, 1991.

(4) Cheeseman, K. H. In *Immunopharmacology of Free Radical Species*; Blake, D., Winyard, P. G., Eds., Academic Press: New York, 1995.

(5) von Sonntag, C. *The Chemical Basis of Radiation Biology*; Taylor and Francis: London, 1987.

(6) Leroy, G.; Sana, M.; Wilante, C. *J. Mol. Struct.* **1991**, *228*, 37−45.

(7) Armstrong, D. A.; Yu, D.; Rauk, A. *Can. J. Chem.* **1996**, *74*, 1192−1199.

(8) Garrison, W. M. *Chem. Rev.* **1987**, *87*, 381−398.

(9) (a) Mieden, O. J.; von Sonntag, C., *Z. Naturforsch.* **1989**, *44b*, 959−974. (b) Mieden, O. J.; von Sonntag, C. *J. Chem. Soc., Perkin. Trans. 2* **1989**, 2071−2078. (c) Mieden, O. J.; von Sonntag, C. *J. Phys. Chem.* **1993**, *97*, 3783−3790.

(10) Stadman, E. R. *Annu. Rev. Biochem.* **1993**, *62*, 797−821.

(11) Rauk, A.; Yu, D.; Armstrong, D. A. *J. Am. Chem. Soc*. **1997**, *119*, 208−217.

10.1021/ja9939688 CCC: $19.00 © 2000 American Chemical Society
Published on Web 04/06/2000

proline,[12] and cysteine.[13] Application of the same methods to the anhydrides of glycine and alanine gave good agreement with experiment.[14] Subsequently, the $^{\alpha}$C−H BDEs of all amino acid residues have been theoretically calculated[15] and predicted to be in the range 330−370 kJ mol^{-1}, low enough for the residues to react with even the milder oxidizing species under circumstances where the residues are exposed and in an unstructured (random coil) environment.

However, real protein structure consists of a complex scaffold, the tertiary structure, assembled from smaller structural units consisting of helices, sheets, and turns, which are in turn assembled from regions of the polypeptide polymer interlinked by H-bonds or disulfide bridges. In previous work,[11−13] the effects of some of these secondary elements on $^{\alpha}$C−H BDEs and activation enthalpies for H-atom transfer have been probed by the simple expedient of imposing constraints in the Φ,Ψ torsion angles. The captodative stabilization[6,7] of the $^{\alpha}$C radical, which underlies the anomalously low BDEs and enthalpies of activation, is diminished as these angles deviate from 180° (coplanarity of the peptide backbone). As a consequence, it was predicted theoretically that the α-helical secondary structure (Φ = −45°,Ψ = −60°) confers protection on the $^{\alpha}$C−H bond toward oxidative damage, but antiparallel β-sheet (Φ = −150°, Ψ = +150°) does not. In the latter case, the BDE rises only by about 10 kJ mol^{-1}. It was argued, but not verified, that the involvement of both the donor and acceptor amide units in H-bonding, should not have a significant effect on BDE. Similarly the activation energy for H-atom abstraction by, say a thiyl or other radical, should parallel the changes in BDE, provided the structure necessary for the transition state could be achieved.

The β-sheet secondary structure is of special significance for two reasons. First, the formation of β-sheet structure in amyloidogenic proteins appears to be a precursor to their damaging role in diseases such as Alzheimer's Disease.[16] Second, as discussed above, the thermochemical barriers to radical formation imposed by the typical range of the Φ,Ψ torsion angles (at least in the antiparallel variation) have been predicted not to be high enough to prevent reaction with reactive oxidizing species (ROS). In the present work, we examine the effect of β-sheet structure on the susceptibility of the $^{\alpha}$C−H site to oxidative damage by explicit calculations on hydrogen bonded dimers of model peptide glycine and alanine units arranged in parallel and antiparallel fashion, with and without imposition of the appropriate β-sheet constraints. The parents and derived radicals are shown in Figure 1, with the specific parent models indicated by the brackets. *Antiparallel* β-sheets have two or more strands in extended conformation with head-to-tail regiochemistry, connected by alternating (3,3) and (5,5) H-bonded networks. Minimization of repulsive interactions between the side chains forces a *pleating* of the sheet with torsion angles, Φ = −150°, Ψ = +150° (approximately, depending on the residues), causing the side chains to be oriented approximately perpendicular to the average plane of the sheet, and the $^{\alpha}$C−H bonds to be pointing toward each other more or less in the plane of the sheet. The adjacent strands of the *parallel* β-sheet run in the same direction and are bound by a repeating

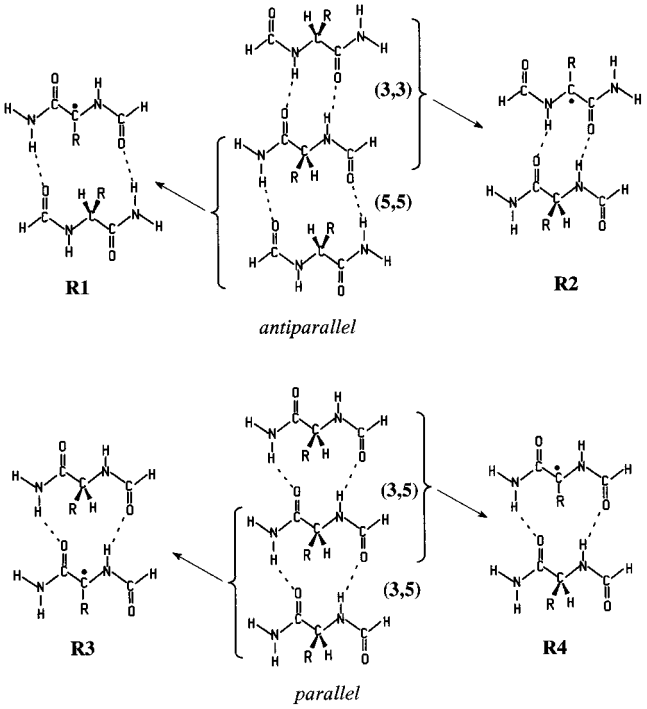

Figure 1. Models for antiparallel and parallel β-sheets: four distinct $^{\alpha}$C radicals arise.

(3,5) network of H-bonds. Accommodation of the H-bonds and side chain repulsions also causes a pleating with smaller torsion angles, Φ = −120°, Ψ = +115° (again approximately, depending on the specific residues).

For either parallel or antiparallel orientation, the disposition of the strand as being on the edge of a sheet or internal to it may be a factor to be considered. Abstraction of either $^{\alpha}$C−H bond of a (5,5) cycle of an antiparallel β-sheet yields a radical of type **R1** (Figure 1), which is characterized by a reorientation of the side chain toward the middle of the cycle. We previously speculated that such reorientation may raise the BDE if the side chain is larger than H.[11] In the case where the strand is internal to the sheet, the radical will also have a (3,3) H-bonding network. Abstraction of an $^{\alpha}$C−H from the "3" bridge of an antiparallel β-sheet also yields this **R1** radical, if the strand is internal to a sheet. A different radical, **R2**, is obtained if the strand is at an edge. In **R2**, the side chain is *exo* to the cycle, oriented to a position unhindered by the presence of an adjacent strand. Another *exo* radical, **R3**, is obtained by abstraction of an $^{\alpha}$C−H from the "3" bridge of a *parallel* β-sheet, provided the strand is at an edge. A fourth radical of type **R4**, is obtained by removal of the $^{\alpha}$C−H bond from the "5" bridge of the (3,5) cycle of the parallel β-sheet.

It is not known to what extent the structural features (principally the Φ,Ψ angles) of the pleated sheets are maintained once the $^{\alpha}$C-centered radical is formed. Some information on this point may be derived by optimization of the H-bonded dimeric structures with and without imposition of the appropriate constraints on the Φ,Ψ torsion angles.

Computational Methods

All calculations were carried out at the B3LYP level of theory using the 6-31G(d) basis set as implemented in the Gaussian 94 and 98 suites of programs.[17] Geometry optimizations were carried out to the point that successive steps produced no more than a 10^{-6} hartree (0.03 kJ mol^{-1}) change in the energy. The $^{\alpha}$C−H BDE for the model **PH**(res) is defined as the heat of reaction 1, $\Delta H_{(1)}°$, where the specific amino acid residue can be indicated by inserting the conventional abbreviation

(12) Block, D. A.; Yu, D.; Armstrong, D. A.; Rauk, A. *Can. J. Chem.* **1998**, *76*, 1042−1049.

(13) Rauk, A.; Yu, D.; Armstrong, D. A. *J. Am. Chem. Soc.* **1998**, *120*, 8848−8855.

(14) Jonsson, M.; Wayner, D. D. M.; Armstrong, D. A.; Yu, D.; Rauk, A. *J. Chem. Soc, Perkin Trans. 2* **1998**, 1967−1972.

(15) Rauk, A.; Yu, D.; Taylor, J.; Shustov, G. V.; Block, D. A.; Armstrong, D. A. *Biochemistry* **1999**, *38*, 9089−9096.

(16) Orpiszewski, J.; Benson, M. D. *J. Mol. Biol.* **1999**, *289*, 413−428.

Table 1. Total Energies and Zero Point Vibrational Energies (ZPVE) of Optimized and β-Sheet-Constrained Structures

structure	type of radical	fully optimized		β-sheet constraints
		E (hartrees)	ZPVE (kJ mol^{-1})	*E* (hartrees)
		Antiparallel (5,5)		
PH(Gly)···**PH**(Gly) **(5,5)**		−755.83504	544.0	−755.83321
$^{\alpha}$**P**$^{\bullet}$(Gly)···**PH**(Gly)	**R1**	−755.19139	509.7	−755.18490
PH(Gly)···**PH**(Ala) **(5,5)**		−795.15134	619.3	−795.15037
$^{\alpha}$**P**$^{\bullet}$(Gly)···**PH**(Ala)	**R1**	−794.50781	584.8	−794.50207
$^{\alpha}$**P**$^{\bullet}$(Ala)···**PH**(Gly)	**R1**	−794.50433	585.3	−794.49999
		Antiparallel (3,3)		
PH(Gly)···**PH**(Gly) **(3,3)**		−755.83444	548.7	−755.81759
$^{\alpha}$**P**$^{\bullet}$(Gly)···**PH**(Gly)	**R2**	−755.19116	511.5	−755.17712
		Parallel (3,5)		
PH(Gly)···**PH**(Gly) **(3,5)**		−755.83518	546.9	−755.82132
$^{\alpha}$**P**$^{\bullet}$(Gly)···**PH**(Gly)	**R3**	−755.19129	511.5	−755.15941
PH(Gly)···$^{\alpha}$**P**$^{\bullet}$(Gly)	**R4**	−755.18876		−755.16446
		Transition Structures (5,5)		
TS($^{\alpha}$**P**$^{\bullet}$(Gly)···**PH**(Gly))		−755.15266	499.5	
TS(**CH$_3$S**$^{\bullet}$**PH**(Gly)···**PH**(Gly))				−1193.87533
TS(**CH$_3$S**$^{\bullet}$**PH**(Gly)···**PH**(Ala))				−1233.19254

(Gly, Ala, etc.) in place of "res" in parentheses. If calculated directly,

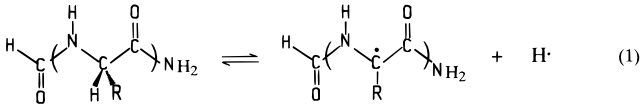

(1)

$\Delta H_{(1)}°$ is subject to a substantial computational error, being calculated to be about 20 kJ mol^{-1} too low. As a means of reducing errors due to basis set and correlation effects, BDEs were derived from the heats of isodesmic reactions.[18] Here reaction 2 was used with H_2NCH_2COOH (D^{α}_{CH} = 331.0 kJ mol^{-1})[7] as the reference molecule, **AH**.

$$^{\alpha}\mathbf{P}^{\bullet}(\text{res}) + \mathbf{AH} \rightleftharpoons \mathbf{PH}(\text{res}) + \mathbf{A}^{\bullet} \quad (2)$$

Then one has:

$$D_{CH}(\mathbf{PH}) = D_{CH}(\mathbf{AH}) - \Delta H_{(2)}° \quad (3)$$

where $\Delta H_{(2)}°$was calculated from the energies of the four species in eq 2 each computed at the B3LYP/6-31G(d) level of theory. This procedure has been shown to yield D_{CH}(**PH**) values with an accuracy within 10 kJ mol^{-1}.[7,14] Structures of several of the most stable conformations of the parent residue model peptide antiparallel and parallel H-bonded dimers and the derived $^{\alpha}$C-centered radicals were obtained. Harmonic vibrational frequency analysis at the B3LYP/6-31G(d) level was performed on the structures optimized with no constraints for the purpose of estimating the zero point vibrational energy (ZPVE). The calculated ZPVE was scaled by 0.98 and assumed to be the same for structures optimized with Φ,Ψ angle constraints.

Transition structures for the transfer of an $^{\alpha}$C−H hydrogen atom to the S atom of a thiyl radical, or to another $^{\alpha}$C-center in the (5,5) cycle of the antiparallel β-sheet were located. Since the device of isodesmic reactions cannot be used directly to reduce errors in the predicted activation parameters, we adjust the potential curve for the reaction to the isodesmically predicted difference in BDEs. Specifically, for both of the cases discussed below, where Φ,Ψ angle constraints are imposed, the calculated endothermicity of the reaction

$$^{\alpha}\text{C}-\text{H} + -\text{S}^{\bullet} \rightarrow \text{TS} \rightarrow {}^{\alpha}\text{C}^{\bullet} + -\text{S}-\text{H}$$

is 12 kJ mol^{-1} higher than the value obtained after isodesmic corrections for the $^{\alpha}$C−H and S−H BDEs were made. We therefore assume that the calculated activation enthalpy is also too high, by *half* this amount, and predict a forward activation enthalpy which is 6 kJ mol^{-1} lower. This procedure has no effect on the calculated enthalpy of activation of H transfer from $^{\alpha}$C to $^{\alpha}$C.

Results

The B3LYP/6-31G(d) energies of all species are collected in Table 1. Selected structures are shown in subsequent Figures beginning in Figure 2. Two derived properties are collected in Table 2, the binding energy, BE, of the dimeric complex (i.e., the energy required to dissociate the complex into monomeric units optimized the same way), and D_{CH}, the $^{\alpha}$C−H bond dissociation enthalpy. Activation parameters for H atom transfer are collected in Table 3.

Discussion

Parent H−Bonded Dimers. Unconstrained Optimizations: Parent Structural Features. Lacking a chiral center, the optimized structure of the glycine model peptide monomer has a planar skeleton and C_s symmetry.[7] The optimized H-bonded dimer in the antiparallel (5,5) cycle, **PH**(Gly)···**PH**(Gly) **(5,5)**, is shown in Figure 2a. The structure is also planar, with D_{2h} symmetry. The NH···O═C separation is 1.96 Å, indicative of a strong H-bond, although the C═O···H angle, 175°, is far from the optimum value (approximately 120°). The two inward-pointing methylene groups are displaced from each other and just out of van der Waals contact. The alanine residue is prototypical of most of the remaining amino acids whose side groups begin with a methylene group. The structure of the **PH**(Gly) moiety in **PH**(Gly)···**PH**(Ala) **(5,5)**, Figure 3a, is almost identical to that in **PH**(Gly)···**PH**(Gly) **(5,5)**, as is the H-bonding network. However, in the **PH**(Ala) of this simple model, the principal features of the pleated antiparallel β-sheet are already apparent, namely the torsion angles, Φ = −154°, Ψ = 159°, which are close to our generic values, and the orientation of the (methyl) side group is perpendicular to the average plane.

(17) Frisch, M. J.; Trucks, G. W.; Schlegel, H. B.; Gill, P. M. W.; Johnson, B. G.; Robb, M. A.; Cheeseman, J. R.; Keith, T. A.; Petersson, G. A.; Montgomery, J. A.; Raghavachari, K.; Al-Laham, M. A.; Zakrewski, V. G.; Ortiz, J. V.; Foresman, J. B.; Cioslowski, J.; Stefanov, B. B.; Nanayakkara, A.; Challacombe, M.; Peng, C. Y.; Ayala, P. Y.; Chen, W.; Wong, M. W.; Andres, J. L.; Replogle, E. S.; Gomperts, R.; Martin, R. L.; Fox, D. J.; Binkley, J. S.; Defrees, D. J.; Baker, J.; Stewart, J. P.; Head-Gordon, M.; Gonzalez, C.; Pople, J. A. *Gaussian 94*, SGI-revision B.3; Gaussian, Inc.: Pittsburgh, PA, 1995.

(18) Hehre, W. J.; Ditchfield, R.; Radom, L.; Pople, J. A. *J. Am. Chem. Soc.* **1970**, *92*, 4796−4816.

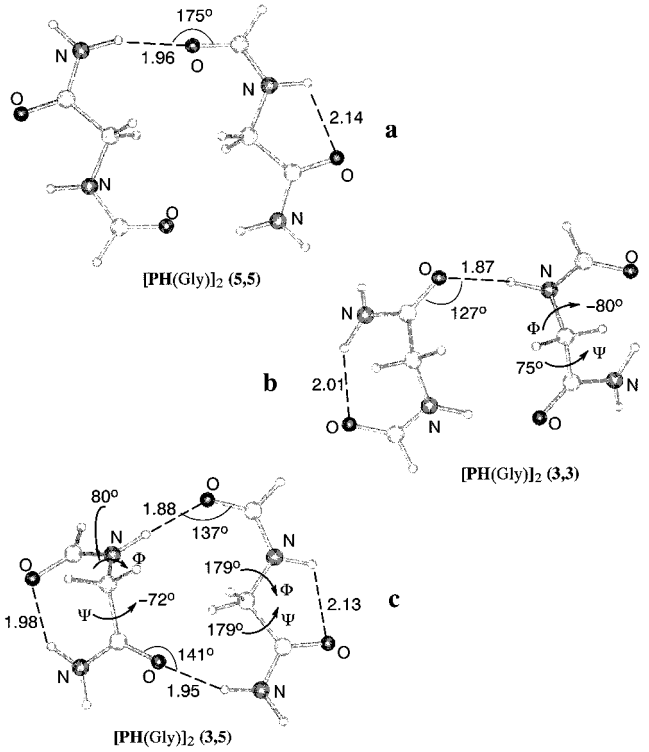

Figure 2. The dimer of **PH**(Gly) fully optimized models for: (a) the (5,5) cycle of an antiparallel β-sheet, (b) the (3,3) cycle of an antiparallel β-sheet, (c) the (3,5) cycle of a parallel β-sheet.

Table 2. Binding Energies, BE, of the H-bonded Complexes and Bond Dissociation Enthalpies, D_{CH}, of the $^{\alpha}$C−H Bonds, in kJ mol^{-1}

structure	type of radical	fully optimized BE	fully optimized D_{CH}	β-sheet constraints BE	β-sheet constraints D_{CH}
Antiparallel (5,5)					
PH(Gly)···**PH**(Gly) **(5,5)**		72.6		74.3	
$^{\alpha}$**P**$^{\bullet}$(Gly)···**PH**(Gly).	**R1**	64.4	358.6	67.6	370.8
PH(Gly)···**PH**(Ala) **(5,5)**		72.2		74.4	
$^{\alpha}$**P**$^{\bullet}$(Gly)···**PH**(Ala)	**R1**	64.5	358.1	67.9	370.6
^{a}**P**$^{\bullet}$(Ala)···**PH**(Gly)	**R1**	49.0	367.7	57.1	376.6
Antiparallel (3,3)					
PH(Gly)···**PH**(Gly) **(3,3)**		66.4		28.7	
$^{\alpha}$**P**$^{\bullet}$(Gly)···**PH**(Gly)	**R2**	62.0	354.8	45.4	347.4
Parallel (3,5)					
PH(Gly)···**PH**(Gly) **(3,5)**		70.2		53.8	
$^{\alpha}$**P**$^{\bullet}$(Gly)···**PH**(Gly)	**R3**	62.4	358.2	52.5	405.5
PH(Gly)···$^{\alpha}$**P**$^{\bullet}$(Gly)	**R4**	55.7	364.8	65.7	389.9

As seen in Figure 2b, The antiparallel (3,3) cycle, unsupported by flanking (5,5) cycles, optimizes to a structure, **PH**(Gly)··· **PH**(Gly) **(3,3)**, with an almost optimum H-bonding network, but at the expense of a highly distorted skeleton with $\Phi = -80°$, $\Psi = 75°$ (or $\Phi = 80°$, $\Psi = -75°$). A similar consequence is seen in the (3,5) cycle of the parallel orientation, **PH**(Gly)··· **PH**(Gly) **(3,5)**, in Figure 2c. The "3" bridge is folded with $\Phi = 80°$, $\Psi = -72°$, and the "5" bridge has an almost planar framework. The H-bond angles at C═O, 137° and 141°, are close to optimum, and as in the (3,3) cycle, the short ═O···H distances are indicative of strong H-bonds. It is apparent that unlike the (5,5) cycle, neither of the fully optimized (3,3) nor (3,5) cyclic structures is compatible with being part of extended β-sheet secondary structure.

Unconstrained Optimizations: Parent Binding Energies. The binding energies, BE, listed in Table 2 are an indication of the strength of the H-bonds. In the fully optimized structures, this is 72 kJ mol^{-1} for the (5,5) cycle, both **PH**(Gly)···**PH**(Gly) and **PH**(Gly)···**PH**(Ala) having virtually the same binding energy. The values listed for the optimized (3,3) and (3,5) cycles are not relevant here since, as noted above, the structures are not compatible with being in an extended β-sheet formation. We return to this point in our discussion of the constrained structures below.

Constrained Optimizations. The structure of **PH**(Gly)··· **PH**(Ala) **(5,5)**, optimized with the torsion angles of both **PH**(Gly) and **PH**(Ala) constrained to the generic antiparallel β-sheet values, $\Phi = -150°$, $\Psi = 150°$, is shown in Figure 3b. The H-bonding network is hardly perturbed by the constraints. The same is true for the parent **PH**(Gly)···**PH**(Gly) in the (5,5) configuration (not shown) but not in the (3,3) and (3,5) configurations which are shown in Figures 4a and 5a, respectively. For the (3,5) cycle, the parallel β-sheet constraints, $\Phi = -120°$, $\Psi = 115°$, were imposed. It is noteworthy that the generic parallel β-sheet torsion angles do not impose as severe a deformation from planarity as that found in the fully optimized structures involving "3" bridges shown in b and c of Figure 2. The BE values of the two constrained (5,5) cyclic structures are again the same, 74 kJ mol^{-1}, and also similar to those found in the unconstrained optimizations. In sharp contrast, the (3,3) cycle has a much lower BE, 29 kJ mol^{-1}. In an extended antiparallel β-sheet, there are equal numbers of (5,5) and (3,3) cycles, suggesting an average binding energy per cycle of 52 kJ mol^{-1}, a value almost identical to that found for the (3,5) cycle, 54 kJ mol^{-1}, which comprises the parallel β-sheet secondary structure.

Radicals. The situation for many of the radicals is more complex than the parents and the properties of the unconstrained and β-sheet-constrained structures are therefore best discussed together.

*Structures of Type **R1**.* The structures of the parent dimers, **PH**(Gly)···**PH**(Gly) **(5,5)** (Figure 2a) and **PH**(Gly)···**PH**(Ala) **(5,5)** (Figure 3a), are hardly perturbed upon conversion of the **PH**(Gly) moiety to the $^{\alpha}$C-centered radical in the absence of β-sheet constraints. The structure of $^{\alpha}$**P**$^{\bullet}$(Gly)···**PH**(Ala) **R1** is shown in Figure 6a. The ═O···H distances are 0.19 Å longer than in the parent, the largest change in torsion angle is 12°, and the frameworks of the two moieties are essentially coplanar. In short, there is room within the (5,5) cycle to accommodate the remaining $^{\alpha}$H atom of the planar $^{\alpha}$C radical site. The same is not true of the methyl group of $^{\alpha}$**P**$^{\bullet}$(Ala) (Figure 6b). To accommodate the planar $^{\alpha}$C radical site, the two components, $^{\alpha}$**P**$^{\bullet}$(Ala) and **PH**(Gly), are forced out of the desirable coplanar arrangement into an almost perpendicular orientation—the angle between the average planes of $^{\alpha}$**P**$^{\bullet}$(Ala) and **PH**(Gly) is about 70°. In addition, both fragments are distinctly nonplanar with torsion angles, $\Phi = -157°$, $\Psi = 170°$ and $\Phi = -158°$, $\Psi = 162°$, respectively.

Generation of a radical site at the $^{\alpha}$C site causes the remaining group at that site to move into the plane, which in the dimer, coincides with the plane of the H-bonding network. Thus, steric considerations will affect the BE of the radical−parent pair. In addition, delocalization of the radical character over the heavy atom skeleton, as represented by the resonance structures shown in Scheme 1, may potentially modify the intrinsic H-bonding characteristics of the radical relative to those of the parent. As can be seen in Table 2, the BE of the unconstrained (5,5) cycles, $^{\alpha}$**P**$^{\bullet}$(Gly)···**PH**(Gly) **R1** and $^{\alpha}$**P**$^{\bullet}$(Gly)···**PH**(Ala) **R1**, are essentially the same, 64 kJ mol^{-1}, but lower by 8 kJ mol^{-1} than that of the parent (5,5) dimers. As expected from the highly distorted structure, the BE of $^{\alpha}$**P**$^{\bullet}$(Ala)···**PH**(Gly) **R1**, 49 kJ

Table 3. Calculated, $\Delta H^{\#}_{calc}$, and Corrected, $\Delta H^{\#}_{Corr}$, Enthalpies of Activation[a]

reaction	$\Delta H^{\#}_{calc}$ (kJ mol^{-1})	$\Delta H^{\#}_{corr}$[b] (kJ mol^{-1})
PH(Gly)···**PH**(Gly) **(5,5)** + $CH_3S^{\bullet}$ → **TS**(**CH$_3$S$^{\bullet}$PH**(Gly)···**PH**(Gly))	39.3	33
$^{\alpha}$**P$^{\bullet}$**(Gly)···**PH**(Gly) **R1** + CH_3SH → **TS**(**CH$_3$S$^{\bullet}$PH**(Gly)···**PH**(Gly))	17.5	23
PH(Gly)···**PH**(Ala) **(5,5)**+ $CH_3S^{\bullet}$ → **TS**(**CH$_3$S$^{\bullet}$PH**(Gly)···**PH**(Ala))	39.2	33
$^{\alpha}$**P$^{\bullet}$**(Gly)···**PH**(Ala) **R1** + CH_3SH → **TS**(**CH$_3$S$^{\bullet}$PH**(Gly)···**PH**(Ala))	17.4	23
$^{\alpha}$**P$^{\bullet}$**(Gly)···**PH**(Gly) **R1** → **TS**($^{\alpha}$**P$^{\bullet}$**(Gly)···**PH**(Gly))	91.7[c] (75)[d]	
$^{\alpha}$**P$^{\bullet}$**(Gly) + **PH**(Gly) → **TS**($^{\alpha}$**P$^{\bullet}$**(Gly)···**PH**(Gly))	27.3[c]	

[a] See Figure 7 for structures of transition states. *β*-Sheet constraints except as noted. [b] Potential curve fitted to difference in $^{\alpha}$C−H and S−H BDEs (see Computational Methods); ΔZPE corrections are adopted from the corresponding monomers (ref 13). [c] Optimized with no constraints. [d] Relative to *β*-sheet constrained dimer.

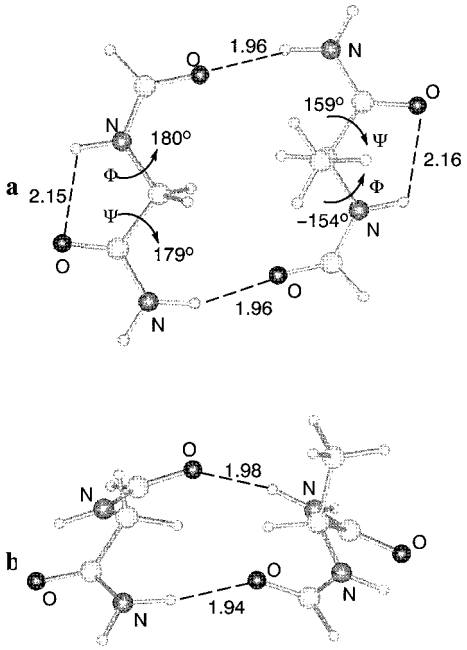

Figure 3. **PH**(Gly)···**PH**(Ala) **(5,5)** optimized with: (a) no constraints, (b) constraints $\Phi = -150°$, $\Psi = 150°$.

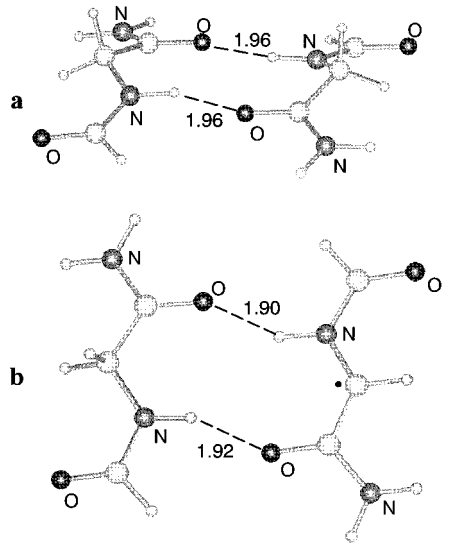

Figure 4. Antiparallel *β*-sheet constraints, $\Phi = -150°$, $\Psi = 150°$: (a) **PH**(Gly)···**PH**(Gly) **(3,3)**, (b) $^{\alpha}$**P$^{\bullet}$**(Gly)···**PH**(Gly) **R2**.

mol^{-1}, is lower by 15 kJ mol^{-1} than that of $^{\alpha}$**P$^{\bullet}$**(Gly)···**PH**(Gly) **R1** or $^{\alpha}$**P$^{\bullet}$**(Gly)···**PH**(Ala) **R1**, and by 23 kJ mol^{-1} relative to the that of the parent.

Imposition of *β*-sheet constraints causes the BE of the (5,5) cycles to increase by 3 kJ mol^{-1} in the case of $^{\alpha}$**P$^{\bullet}$**(Gly)···**PH**(Gly) **R1** and $^{\alpha}$**P$^{\bullet}$**(Gly)···**PH**(Ala) **R1**, and by 8 kJ mol^{-1} in the case of $^{\alpha}$**P$^{\bullet}$**(Ala)···**PH**(Gly) **R1** (see Table 2). These small effects are in accord with the minor structural changes caused by these constraints.

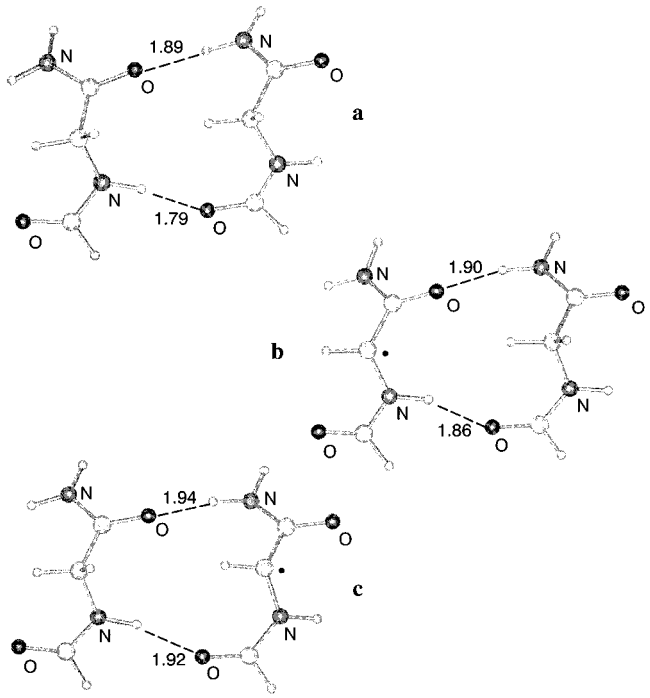

Figure 5. Parallel *β*-sheet constraints, $\Phi = -120°$, $\Psi = 115°$: (a) **PH**(Gly)···**PH**(Gly) **(3,5)**, (b) $^{\alpha}$**P$^{\bullet}$**(Gly)···**PH**(Gly) **R3**, (c) **PH**(Gly)···$^{\alpha}$**P$^{\bullet}$**(Gly) **R4**.

*Structures of Type **R2***. The situation is more complicated for the antiparallel (3,3) cycle, $^{\alpha}$**P$^{\bullet}$**(Gly)···**PH**(Gly) **R2**. The optimized structure is not shown but, as in the case of the parent system (Figure 2b), optimization without constraints results in a buckled structure for the **PH**(Gly) moiety and the formation of an additional intraresidue H-bond which is not possible as part of *β*-sheet structure. However, the radical fragment, $^{\alpha}$**P$^{\bullet}$**-(Gly), optimized to a planar structure. One would expect this to be the case even if the adjacent strand were constrained to *β*-sheet torsion angles, a fact that is confirmed by the *β*-sheet-constrained structure of $^{\alpha}$**P$^{\bullet}$**(Gly)···**PH**(Gly) **R2** in Figure 4b which is relatively unperturbed from that of the parent. The binding energy is 17 kJ mol^{-1} higher than the parent (Figure 4a). Steric factors are not important for either species so one must attribute the stronger H-bonds to electronic effects. The shorter ═O···H distances support this view. Note that radicals of type R2 differ from type R1 in that they are at an edge of the *β*-sheet. Steric considerations that are important for type R1, as demonstrated in the case of $^{\alpha}$**P$^{\bullet}$**(Ala)···**PH**(Gly) **R1** discussed above, do not apply for type R2.

*Structures of Types **R3** and **R4***. The structures of the parallel (3,5) cycle, $^{\alpha}$**P$^{\bullet}$**(Gly)···**PH**(Gly) **R3**, (at the "3" bridge),

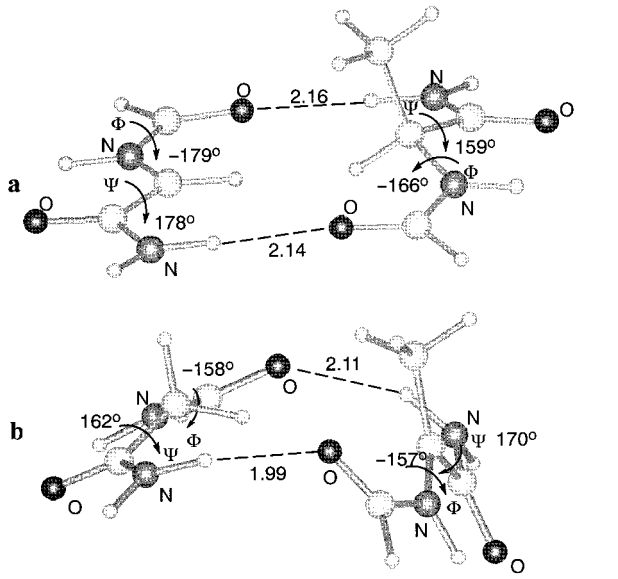

Figure 6. Unconstrained type **R1** radicals: (a) $^{\alpha}$**P**$^{\bullet}$(Gly)$\cdots$**PH**(Ala), (b) $^{\alpha}$**P**$^{\bullet}$(Ala)$\cdots$**PH**(Gly).

Scheme 1

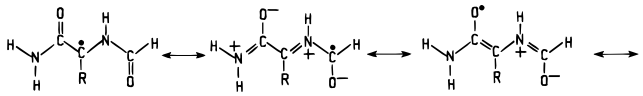

and $^{\alpha}$**P**$^{\bullet}$(Gly)$\cdots$**PH**(Gly) **R4**, (at the "5" bridge), with torsion angles constrained to parallel β-sheet values, are shown in Figure 5, parts b and c, respectively. The $=$O$\cdots$H bond distances of the former are slightly shorter although the BE of the latter is greater by 13 kJ mol^{-1}, and greater by 12 kJ mol^{-1} than that of the parent (Figure 5a). Unconstrained optimization of $^{\alpha}$**P**$^{\bullet}$(Gly)$\cdot\cdot$**PH**(Gly) **R3** yields a planar structure for the cycle, with C_s symmetry, while only the $^{\alpha}$**P**$^{\bullet}$(Gly) component of $^{\alpha}$**P**$^{\bullet}$(Gly)$\cdots$**PH**(Gly) **R4** is planar. It is noted again that the type R3 radical is at an edge of the parallel β-sheet. Thus, the in-plane position of a side chain of a residue other than glycine does not pose steric problems. However, type R4 radicals, like R1, will face severe steric hindrance in positioning the side chain. This is expected to be even more severe (given that a (3,5) cycle has a smaller interior cavity than a (5,5) cycle), but we did not test this hypothesis with an alanine residue, as in the case of $^{\alpha}$**P**$^{\bullet}$-(Ala)$\cdots$**PH**(Gly) **R1**.

$^{\alpha}$C−H Bond Dissociation Enthalpies, D_{CH}. Values of D_{CH} obtained by both β-sheet constrained and unconstrained optimizations are listed in Table 2. A quick perusal reveals that D_{CH} for glycine in the fully optimized structures fall in the narrow range 355−365 kJ mol^{-1} for the fully optimized H-bonded structures. These values are to be compared with 350 kJ mol^{-1}, the value of D_{CH} for isolated **PH**(Gly).[7] An immediate first conclusion is that H-bonding to a neighboring strand increases the bond strength of the $^{\alpha}$C−H bond by a modest 5−15 kJ mol^{-1} through electronic and/or steric effects. For the alanyl radical, the latter effect is obviously the principal component of the increase in D_{CH} of the $^{\alpha}$C−H bond—the optimized value in Table 2, 368 kJ mol^{-1}, is 23 kJ mol^{-1} higher than the value derived for isolated **PH**(Ala), 345 kJ mol^{-1}.[11] As was found in the case of BE values, comparison of D_{CH} of the **PH**(Gly) parts of **PH**(Gly)$\cdots$**PH**(Gly) **(5,5)** and **PH**(Gly)$\cdot\cdot$**PH**(Ala) **(5,5)** suggests that the strength of the $^{\alpha}$C−H bond is independent of the cross-ring residue in a (5,5) cycle. The same is true when the structures are constrained to having β-sheet torsion angles. The effect of the constraint though is to increase D_{CH} by a further 12 kJ mol^{-1} to 371 kJ mol^{-1}. In isolated PH-(Gly) with the same β-sheet constraints, D_{CH} = 361 kJ mol^{-1}.[11] Thus, the effect of H-bonding is to raise D_{CH} by a small amount. It is likely that D_{CH} of the glycyl residue in an antiparallel β-sheet will be somewhat less than 371 kJ mol^{-1}, since some relaxation[19] of the radical structure will take place even though its cross-ring partner is held in place by the rest of the β-sheet network. Thus, the $^{\alpha}$C−H bond strength of the glycine residue in such an environment is comparable to that of a sulfhydryl S−H bond (367 kJ mol^{-1}),[13] and the conclusion is that it is thermodynamically feasible for a thiyl radical (RS$^{\bullet}$) to exchange a H atom with a glycyl $^{\alpha}$C-centered radical. We examine the question of kinetic feasibility, that is, the activation energy for the process, below.

We note that in the case of the (3,3) cycle yielding the β-sheet-constrained edge-positioned type R2 radical, $^{\alpha}$**P**$^{\bullet}$(Gly)$\cdot\cdot\cdot$**PH**(Gly) **R2**, D_{CH} = 347 kJ mol^{-1} (Table 2). This value is lower by 14 kJ mol^{-1} than that of the the similarly constrained but isolated peptide, **PH**(Gly). Thus, in this case, H-bonding to the C$=$O and N−H immediately flanking the formal radical site lowers the strength of the $^{\alpha}$C−H bond. This consequence may be due to a significant contribution of the middle resonance structure shown in Scheme 1. Again, the ability to relax the radical somewhat may lower this value even further. These considerations may apply to most other amino acid residues at the edges of antiparallel β-sheets, since steric factors are less important. Thus, the edge strand of an antiparallel β-sheet may be particularly susceptible to oxidative damage at the outside "3" position of a (3,3) cycle.

The Parallel β-Sheet. The angular constraints, $\Phi = -120°$, $\Psi = 115°$, of a parallel β-sheet raise the energy of the parent (monomeric) system, **PH**(Gly), by a modest 10 kJ mol^{-1}, but they have a much larger effect on the radical $^{\alpha}$**P**$^{\bullet}$(Gly), raising its energy by 64 kJ mol^{-1}. The difference translates directly into an increase in bond strength, D_{CH} = 404 kJ mol^{-1}.[20] In effect, all captodative stabilization of the radical is lost upon such severe deformation from planarity. This consequence is also seen in the data on the β-sheet constrained (3,5) cycles in Table 2. D_{CH} = 406 kJ mol^{-1} at the "3" bridge, and D_{CH} = 390 kJ mol^{-1} at the "5" bridge. Relaxation of the radical moiety will lower these values to some extent. However, it is unlikely that they will approach the bond strength of the RS−H bond. Thus the $^{\alpha}$C−H bond of glycine, and presumably any other residue, in a parallel β-sheet is too strong to be damaged by the weaker oxidizing radicals such as RS$^{\bullet}$, ROO$^{\bullet}$, and $O_2^{\bullet-}$.

Activation Energies: Reaction with Thiyl Radicals. We have previously predicted that thiyl radicals, modeled by $CH_3S^{\bullet}$, are able to abstract a H atom from isolated **PH**(Gly) with enthalpy of activation of 27 kJ mol^{-1}.[13] The transition structures for the reaction of $CH_3S^{\bullet}$ with **PH**(Gly)$\cdots$**PH**(Gly) **(5,5)** and **PH**(Gly)$\cdot\cdot$**PH**(Ala) **(5,5)** at the glycyl site, optimized with the β-sheet constraints, are shown in Figure 7, parts a and b, respectively. The geometric parameters of the two are almost identical, showing little perturbation by the presence of the methyl group. The H atom is almost midway between the S and $^{\alpha}$C centers. This corresponds to a proportionally greater stretch of the $^{\alpha}$C−H bond and a late transition state. Enthalpies

(19) Even in secondary structure, the parent residues should exist in conformations close to their optimum. However, the optimum geometry of the $^{\alpha}$C radical is significantly different from that of the parent, and some shift toward the optimum value will occur despite constraints imposed by secondary structure. Such "relaxation" is not permitted in our torsion angle constrained optimizations, and thus an upper limit of the $^{\alpha}$C−H BDE is expected.

(20) Rauk, A.; Armstrong, D. A. Unpublished results.

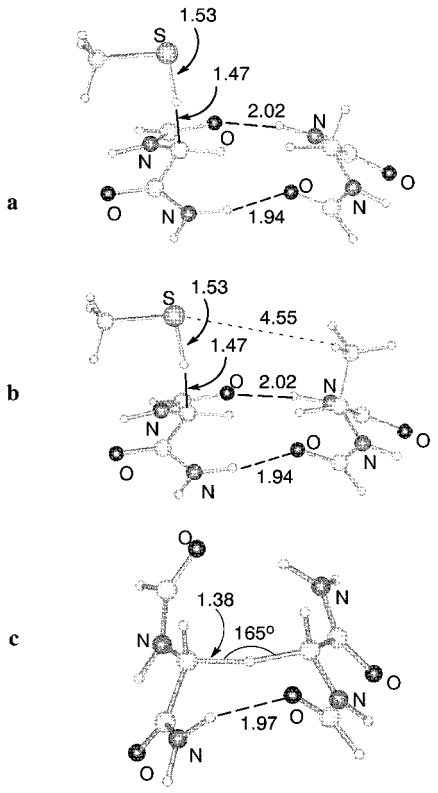

Figure 7. Transition structures: (a) **TS**(**CH$_3$S$^\bullet$PH**(Gly)···**PH**(Gly)), (b) **TS**(**CH$_3$S$^\bullet$PH**(Gly)···**PH**(Ala)), (c) **TS**($^\alpha$**P$^\bullet$**(Gly)···**PH**(Gly)).

of activation are listed in Table 3. The enthalpy of activation of the forward reaction,

$$CH_3S^\bullet + \mathbf{PH}(\mathrm{Gly})\cdots\mathbf{PH}(\mathrm{res}) \rightarrow CH_3SH + {}^\alpha\mathbf{P}^\bullet(\mathrm{Gly})\cdots\mathbf{PH}(\mathrm{res})$$

where res = Gly or Ala, is 33 kJ mol^{-1} for both systems, after adjustment for the fact that the reaction is endothermic by 10 kJ mol^{-1} in each case. Thus, the activation energy for the H atom abstraction is predicted to be only 6 kJ mol^{-1} higher for the antiparallel β-sheet structure than for a glycyl residue in a random coil environment.[13] The activation enthalpy for the reverse step is 23 kJ mol^{-1}. In the anaerobic enzyme systems, *Escherichia coli* ribonucleotide reductase (RNR) and pyruvate formate lyase (PFL), and bacteriophage T4 RNR, the reversible transfer of a hydrogen atom between thiyl (cysteinyl) and glycyl residues forms part of the normal functioning of the enzyme.[21] The structures of two of the three enzymes are known from X-ray crystallography.[22] In each case, the active-site Gly residue is at the top of a hairpin loop, and nonplanar. However, electron spin resonance measurements indicate that the glycyl radical of the activated enzyme has relaxed to a planar geometry in the *E. coli* enzymes but is still nonplanar in T4 RNR.[23] While the present paper deals with β-sheet secondary structure and not the hairpin loop, the present results imply that the nonplanarity and H-bonding inherent in this structure would narrow the energy difference between $^\alpha$C−H and S−H BDEs and facilitate the reversible H atom transfer.

Activation Energies: Chain to Chain propagation. The data in Table 3 and the transition structure shown in Figure 7c are pertinent to the question, "Once formed, how easy is it for damage to migrate from one $^\alpha$C-site to another?" The structure of the fully optimized TS, **TS**($^\alpha$**P$^\bullet$**(Gly)···**PH**(Gly)), represents the critical stage for migration of the H atom from an intact glycyl residue to the $^\alpha$C-centered radical site of another. The structure is C_2 symmetric as a consequence of the antiparallel regiochemistry. If one considers **TS**($^\alpha$**P$^\bullet$**(Gly)···**PH**(Gly)) to be the TS for propagation of damage from an unconstrained R1 radical across the (5,5) cycle, it is evident that the normal H-bonding framework of the (5,5) cycle is completely disrupted, although some attraction is evident in the short ═O···H distances (1.97 Å). The enthalpy of activation is predicted to be 92 kJ mol^{-1}. If one starts from the β-sheet-constrained R1 structure, the activation enthalpy is 75 kJ mol^{-1}. In view of the high enthalpies of activation, one must conclude that it is not feasible to propagate radical damage from one strand to another within the same β-sheet.

One may also view **TS**($^\alpha$**P$^\bullet$**(Gly)···**PH**(Gly)) as representative of the TS for H-atom transfer between isolated strands of random coil. In this case, the enthalpy of activation is predicted to be 27 kJ mol^{-1} (i.e., relative to $^\alpha$**P$^\bullet$**(Gly) + **PH**(Gly)), low enough to permit rapid migration of damage. A similar activation energy is expected for most pairs of residues. In principle, steric considerations are not important in this "intermolecular" case, but rather the relative strengths of the $^\alpha$C−H bonds of the two residues, almost all of which are similar to, or smaller than, D_{CH} of **PH**(Gly).[15] Thus, in the case of a random coil, it would appear that damage can propagate to any residue other than proline which has too strong a $^\alpha$C−H bond.[15] **TS**($^\alpha$**P$^\bullet$**(Gly)···**PH**(Gly)) should also be representative of the TS for H-atom transfer from $^\alpha$**P$^\bullet$**(Gly) on one strand of a β-sheet to any nonproline residue of a random coil strand, or from one β-sheet to a second overlaying antiparallel β-sheet. In the last case, the two residues involved are necessarily glycine residues.

Conclusions

The present results suggest that:

- the presence of a H-bonded strand of an *antiparallel* β-sheet has only a modest effect on the $^\alpha$C−H BDE of a glycine residue but raises the BDE of other residues by a significant amount if they are part of a (5,5) cycle;

- the *parallel* β-sheet structure and Φ,Ψ angles lead to a significant increase in BDE due to loss of captodative stabilization;

- the *antiparallel* β-sheet structure and Φ,Ψ angles do not lead to a significant increase in BDE relative to the random coil structure;

- all residues incorporated in β-sheet secondary structure, with the exception of glycine, are protected from oxidative damage because the $^\alpha$C−H bond is internal to the sheet and inaccessible to oxidizing radicals;

- glycine is susceptible to oxidative damage because it has a second $^\alpha$C−H bond which is exposed;

- among residues in secondary structure, only glycine is susceptible to damage by weak oxidants such as thiyl, peroxyl, and superoxide, provided it is in an antiparallel β-sheet;

(21) Brush, E. J.; Lipsett, K. A.; Kozarich, J. W. *Biochemistry* **1988**, *27*, 2217−2222.

(22) (a) G580A mutant of T4 RNR (nrdD): Logan, D. T.; Andersson, J.; Sjöberg, B.-M.; Nordlund, P. *Science* **1999**, *283*, 1499−1504. (b) Wild-type unactivated PFL: Becker, A.; Fritz-Wolf, K.; Kabsch, W.; Knappe, J.; Schultz, S.; Wagner, A. F. W. *Nat. Struct. Biol.* **1999**, *6*, 969−975. (c) truncated PFL missing active site Gly: Leppänen, V.-M.; Merckel, M. C.; Ollis, D. L.; Wong, K. K.; Kozarich, J. W.; Goldman, A. *Structure* **1999**, *7*, 733−744.

(23) Himo, F.; Eriksson, L. A. *J. Chem. Soc., Perkin Trans. 2* **1998**, 305−308.

- radical damage may propagate readily from one strand to another above the β-sheet but not within the β-sheet;

- β-sheet structure narrows the difference between the glycyl $^{\alpha}$C−H BDE and S−H BDE and facilitates interstrand H atom transfer between the glycyl $^{\alpha}$C site and the S atom of cysteine.

Acknowledgment. The financial assistance of the Natural Sciences and Engineering Research Council of Canada is gratefully acknowledged.

JA9939688